Conformational photoswitching of a synthetic peptide foldamer bound within a phospholipid bilayer

Matteo De Poli[1], Wojciech Zawodny[1], Ophélie Quinonero[1], Mark Lorch[2], Simon J. Webb[1,3], Jonathan Clayden[4]*

[1]School of Chemistry, University of Manchester, Oxford Road, Manchester M13 9PL, UK.

[2]Department of Chemistry, University of Hull, Cottingham Road, Hull HU6 7RX, UK.

[3]Manchester Institute of Biotechnology, University of Manchester, 131 Princess Street, Manchester M1 7DN, UK.

[4]School of Chemistry, University of Bristol, Cantock's Close, Bristol BS8 1TS, UK.

*Correspondence to: j.clayden@bristol.ac.uk

Abstract: The dynamic properties of foldamers, synthetic molecules that mimic folded biomolecules, have mainly been explored in free solution. Here we report on the design, synthesis, and conformational behavior of photoresponsive foldamers bound in a phospholipid bilayer akin to a biological membrane phase. These molecules contain a chromophore, which can be switched between two configurations by different wavelengths of light, attached to a helical oligoamide that both promotes membrane insertion and communicates conformational change along its length. Light-induced structural changes in the chromophore are translated into global conformational changes, detected by monitoring the solid state ^{19}F nuclear magnetic resonance signals of a remote fluorine-containing residue located 1 to 2 nm away. The behavior of the foldamers in the membrane phase is similar to that of analogous compounds in organic solvents.

One Sentence Summary:

A membrane-bound synthetic molecule communicates photochemical information across nanometer-scale distances within a phospholipid bilayer.

Substantial progress has been made in the field of synthetic biology in the use of light to control biological function by customization of membrane-bound proteins with artificial chromophores (*1*). In parallel, synthetic molecular photoswitches have been used to control chemical processes such as ligand binding and catalysis in isotropic solution (*2, 3*). Here we report the design and synthesis of a fully synthetic photoresponsive helical molecule that can insert into a phospholipid bilayer. We show that light-induced switching between configurational isomers can be used to induce global conformational change that propagates over several nanometers in a synthetic molecule within a membrane environment. Artificial membrane-bound photoswitchable synthetic structures capable of translating photochemical information into extended conformational changes, in a manner reminiscent of the operation of natural photoswitchable proteins such as rhodopsin (*4*), could ultimately provide opportunities for

controlling chemical processes within membrane-defined compartments. Detailed understanding of the way that the phospholipid bilayer affects long-range conformational changes in membrane-bound molecules is limited by the difficulty of observing directly conformational changes in the membrane phase and by a lack of examples of biomolecules that adopt well defined structures in both the membrane phase and in solution (*5, 6, 7*). A simplified yet functional synthetic analogue of the membrane-spanning domains of natural proteins, containing in-built spectroscopic handles that are diagnostic of conformation, would be a powerful tool. Dynamic conformational changes in a membrane-bound molecule could then be explored, free of the complexities of protein structure, and compared with analogous changes in isotropic solution.

Given the requirement for a synthetic structure with a tendency to embed into membranes and with well-understood conformational dynamics, we chose to explore the membrane insertion of foldamers (synthetic polymeric molecules with well defined conformations (*8*)) built from oligomers of the achiral amino acid Aib (2-aminoisobutyric acid, Figure 1A, shown in black). These Aib foldamers show a strong preference for helical conformations (*9*) and therefore have two principal conformational states, in which the helix adopts a global left or right-handed screw sense. Furthermore, helical Aib-rich peptides have a known tendency to insert into phospholipid bilayers because they occur naturally in the form of membrane-disrupting fungal antibiotics known as peptaibols (*10*).

In order to allow photochemical induction of conformational change, a chiral amino acid residue was covalently linked to the N-terminus of an $(Aib)_n$ foldamer and then N-acylated by an azobenzene motif (shown in red in Fig. 1A) (*11*). This motif manifests well understood photochemical interconversion between *E* and *Z* configurations and thus offers a reversible light-driven means of initiating conformational re-organization from the terminus of the oligomer. The influence of azobenzene geometry on the relative population of conformational states of the $(Aib)_n$ helix was first explored in solution using foldamers **1** (Fig. 1A) that carry a C-terminal glycinamide as a solution-state ^{1}H NMR-compatible reporter of helical conformation (*12*). An unequal conformational population can result when the first turn of a helical Aib-containing foldamer incorporates a single chiral tertiary amino acid residue, and the magnitude of this bias depends on the detailed structure of the first (N-terminal) β-turn of the helix (*12*). ^{1}H NMR spectra of valine-containing foldamers **1a-d** were acquired in deuterated methanol (CD_3OD) solution as their thermally equilibrated mixtures of *E* (major) and *Z* (minor) geometrical isomers (analogous behavior in phenylalanine-containing foldamers is reported in table S1). Methanol has a polarity similar to the interfacial region of the phospholipid bilayer and prevents aggregation of the foldamers in solution (*13, 14*). Since the left- and right-handed conformational states of an $(Aib)_n$ helix interconvert on a sub-millisecond timescale at ambient temperature, the ^{1}H NMR spectrum that is observed results from a weighted average of both conformational states, reflecting their relative population. The diagnostic feature in the averaged spectra of foldamers **1** is the signal or signals due to the methylene protons of the C-terminal glycinamide residue. A single signal indicates equal population of the two states; a pair of signals indicates unequally populated states. Furthermore, the magnitude of the chemical shift difference $\Delta\delta$ between these signals is proportional to the excess population of one screw-sense conformation over the other. A change in $\Delta\delta$ therefore indicates a change in population distribution across these two conformational states (*12*).

A comparison of the chemical shift differences $\Delta\delta$ in the glycinamide residue of the *E* and the *Z* geometrical isomers of **1a-d** (Fig. 1B) showed that the *E* isomers consistently exhibited greater $\Delta\delta$ values than the *Z* isomers. This indicates that the *E* isomer of the azobenzene induces

a more powerful conformational preference K_E than that of the Z isomer K_Z, and induces a more unequal distribution of screw-sense populations (Fig. 1A-C). The sensitivity of the conformational preference of **1** to the geometry of the azobenzene was tuned by varying the substituent in the *meta* position of the terminal ring (*15*, *16*). Methoxy-substituted **1c** and **1d** showed the greatest differences in conformational populations between their E and Z isomers (Fig 1C), and were cleanly photoswitched from E to Z on irradiation at 365 nm and from Z to E on irradiation at 455 nm (fig. S2). Both **1c** and **1d** exhibited particularly slow thermal relaxation from Z to E [$t_{1/2}$ of 64 h for **1d** (fig. S6)], and the *para*-fluoro substituent of **1d** additionally provided a local ^{19}F NMR reporter of azobenzene geometry.
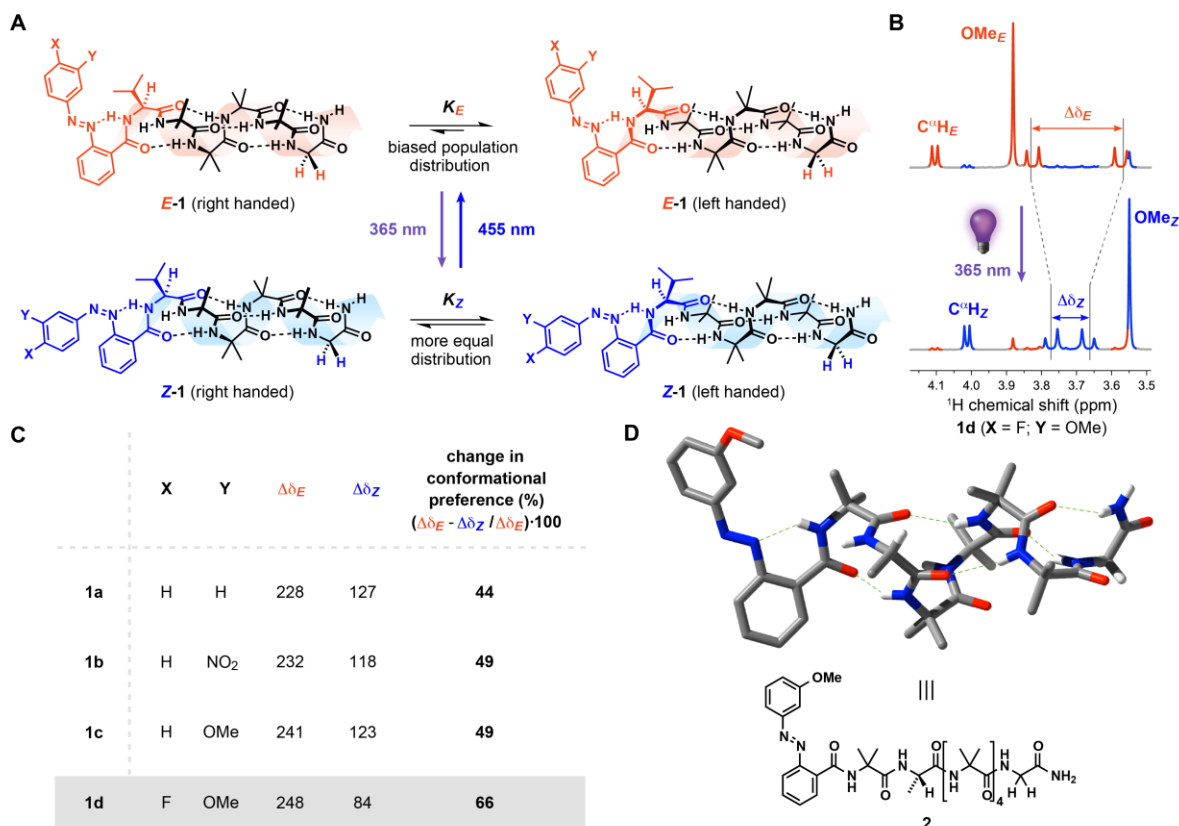

Fig. 1. Validation of the photoswitchable foldamer architecture **1** in solution. (A) Switching the terminal azobenzene chromophore between E and Z configurations changes the population distribution between right-handed and left-handed conformations of foldamers **1a-d** with general structure Azo-Val-Aib$_4$-GlyNH$_2$; (B) Portions of ^{1}H NMR spectra showing the change in chemical shift separation $\Delta\delta$ between the signals arising from the glycinamide methylene protons of foldamer **1d** in CD$_3$OD upon irradiation with light of 365 nm; (C) Percentage change in population distribution for foldamers **1a-d**, calculated from $\Delta\delta$ values; (D) The intramolecular hydrogen bonding network (shown in green) in the X-ray crystal structure of Azo-Aib-Ala-Aib$_4$-GlyNH$_2$ **2**.

We assume that the conformational switching of **1** is driven by a difference in electronic properties between the E and Z azobenzene-2-carboxamides. The population distribution

between screw-sense conformations across a series of related (Aib)$_n$ foldamers is sensitive to the basicity of the carbonyl group linked to the N-terminal residue that initiates the first β-turn of the helix (*12*). The X-ray crystal structure of an azobenzene-2-carboxamide capped foldamer **2** (Fig. 1D) reveals that the proximal azo nitrogen atom forms an intramolecular hydrogen bond in the solid state with the NH of this N-terminal residue. Given the persistence of the intramolecular hydrogen bond network of Aib foldamers even in polar, hydrogen-bonding solvents (*17*), we assume this hydrogen bond is retained in solution. On photoisomerization from *E* to *Z*, the azobenzene loses planarity and the diazo group becomes more basic (*18*), likely strengthening this hydrogen bond, and in turn altering the geometry of the hydrogen bonding and hence the conformational preference within the β-turn. This change in conformational preference is propagated through the helical chain, leading to a detectable shift in the relative populations of left-and right-handed helical conformations, reported by the ^{1}H NMR signals of the C-terminal glycinamide reporter.

Having established that the conformational populations of the foldamers in solution could be perturbed by photochemical switching and detected by solution state ^{1}H NMR, we needed to devise a means of detecting conformational changes in related foldamers when embedded in a membrane. Solid state nuclear magnetic resonance (ss-NMR (*19*)) is a powerful analytical technique that can determine structures in non-dissolved systems with quasi-atomic resolution. It can be used to characterize membrane-bound structures (*20, 21*), and it can yield detailed information on the conformation and dynamics of membrane-bound proteins and peptides (*22, 23, 24*) and their artificial mimics (*25*). It has recently been used to investigate both the structure and dynamics of the photoswitchable vision protein rhodopsin (*26*), and provides evidence that the solution-phase conformational preference of the Aib-rich peptaibol alamethicin is preserved when embedded in phospholipid bilayers (*27*). Magic angle spinning (MAS) is the most commonly used ss-NMR method (*28*), and in a lipid bilayer, MAS spin rates of ~10 kHz generate well resolved ^{1}H ss-NMR signals within an experimental time scale of 1 h (*29*). In the H, C and P-rich membrane environment, details of orientation, conformation, folding and association can be obtained through incorporation of fluorine substituents into natural (*30*) and artificial molecules (*31*). Temperature, drug and solvation-dependent conformational changes of labeled membrane-bound proteins have been detected by ss-NMR (*32*) but the method has rarely been used to quantify conformational ratios or to observe dynamic conformational changes in artificial membrane-bound molecules (*33*).

In order to identify the foldamer in the phospholipid bilayer we incorporated into its structure a 2,2-difluoroAib (Fib (*34*)) residue (Fig. 2, shown in green). Located at the foldamer's C-terminus, several nanometers remote from the chromophore, Fib's pair of fluorine atoms allow the use of ^{19}F ss-NMR (*30, 35*) to detect changes in the conformational population distributions, since chemical shift differences (Δδ) between the ^{19}F NMR signals of the two fluorine atoms of 2,2-difluoroAib (Fib) report on the conformational preferences of helical foldamers in solution in a similar way to the glycinamide probe of **1** (*34*). Initially, a series of foldamers **3a-f** (Fig. 2) lacking the azobenzene chromophore was synthesized in order to validate the use of Fib as a conformational reporter in the membrane phase. To enhance membrane solubility, a triethyleneglycol (TEG) tail was ligated to the C terminus of the foldamers, adjacent to the Fib residue. The spatial separation between the FibTEG reporter and the N-terminal chiral residue ensures the chemical shift difference Δδ between the ^{19}F NMR signals is insensitive to configurational changes in the chromophore, and thus reports only on induced conformational changes in the helical part of the foldamer. The ^{19}F NMR spectra of foldamers **3a-f** in

trideuterated methanol (CD$_3$OH) at 23 °C showed pairs of signals with chemical shift differences $\Delta\delta$ that are proportional to the screw-sense population distributions reported for related compounds (*12*). The $\Delta\delta$ value provides a measure of population distribution between conformations only when exchange between screw-senses is fast on the NMR time scale, so variable temperature ^{19}F NMR (fig. S7) was used to confirm that the conformations of **3a** interconvert rapidly (i.e. at a rate of >6000 s^{-1}) in both CD$_3$OH (coalescence temperature T_c of **3a** = 0 °C) and deuteriochloroform (CDCl$_3$, T_c of **3a** = +7 °C), a low dielectric constant solvent that simulates the low polarity at the center of a phospholipid bilayer (*36*).

The dynamic conformational behavior of the helical foldamers **3** was then studied in a membrane environment using ss-NMR. Multilamellar vesicles (MLVs, (*37*)) were prepared by co-dissolving **3** and the phospholipid 1,2-dioleoyl-*sn*-glycero-3-phosphocholine (DOPC) (1:19-1:9 peptide/DOPC w/w ratio) in chloroform (*38*). After removal of solvent under reduced pressure, the residue was rehydrated, freeze-dried and resuspended in phosphate buffer solution (pH 7.2). Centrifugation and removal of the aqueous supernatant layer afforded a viscous lipid phase which was loaded into a MAS zirconia rotor (fig. S6). The ^{31}P static NMR spectrum showed an anisotropic signal, while the ^{1}H MAS ss-NMR spectrum showed resolved, sharp peaks from both the lipids and foldamer (see fig. S7), indicative of a lipidic fluid lamellar phase into which the oligomer is embedded but remains freely mobile (*39, 40, 41*).

^{19}F MAS ss-NMR spectra of **3a-f** embedded in DOPC membranes were acquired with a spinning rate of 10 kHz, and were compared with solution phase ^{19}F NMR spectra of the same compounds **3a-f** in CD$_3$OH (Fig. 2). In every case, either one or two ^{19}F signals centered around δ −234 ppm were observed in the ss-NMR spectrum, further confirming that the fluorinated foldamers **3a-f** had partitioned into the lipid bilayer. The single ^{19}F NMR signal of the achiral foldamer **3a** both in solution phase NMR and ss-NMR suggested that the rapid screw-sense inversion observed in solution persists in the membrane phase, allowing use of chemical shift differences $\Delta\delta$ in the ^{19}F ss-NMR spectrum to measure the population distribution of helical conformations in the membrane. The increasing separation of the ^{19}F NMR signals of the FibTEG probe in the series **3b-f** in both solution and solid state confirms the increasingly strong chiral influence at the remote N-terminus in both environments. Strongly helicogenic, C$^\alpha$-tetrasubstituted residues (α-methylvaline, aMv), and in particular two consecutive aMv residues, induced the greatest bias in the conformational population in both environments. Although some subtle differences are evident, probably due to a weakening of conformational induction in a membrane environment, the similar conformational behavior of **3a-f** both in isotropic solution and in the liquid crystal (*42*) environment of the DOPC bilayer suggests that the population of foldamer conformations in the membrane phase may be predicted by studying their population distribution in solution. ^{19}F ss-NMR spectra were concentration-independent: there was no change in $\Delta\delta$ on varying the loading of foldamer **3d** from 3 to 15% w/w (see fig. S12), nor on adding a non-fluorinated, chiral foldamer to a lipid bilayer already containing **3d** (fig. S13), indicating that screw-sense preferences detected by ^{19}F ss-NMR are not the result of intermolecular communication between helices. The single ^{19}F ss-NMR signal of **3a** confirms that the chirality of DOPC has no discernible influence on screw-sense preference.
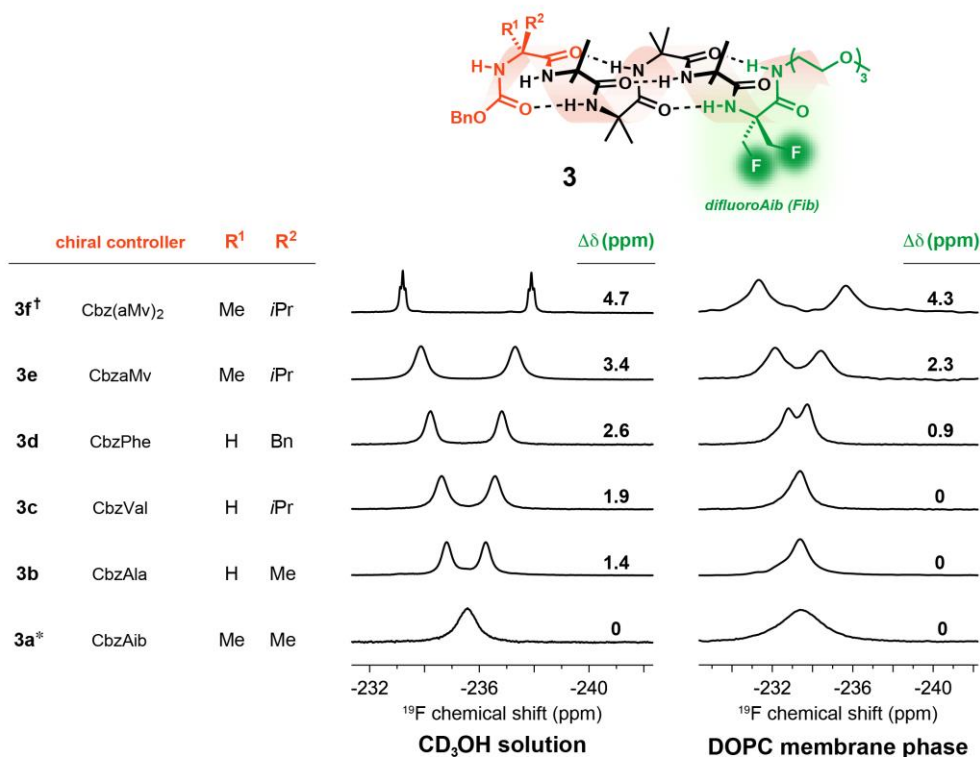
Fig. 2. Solution and membrane-phase ^{19}F NMR signals of fluorinated foldamers **3a-f** along with their corresponding chemical shift separations Δδ. aMv = L-α-methylvaline. (*) Achiral residue; (†) Two consecutive aMv residues.

Having shown that the constituent parts function successfully in isolation, we brought them together in the synthesis of a foldamer designed for photoswitching in the membrane phase. The most effective azobenzene motif **1d** (Fig. 1) was ligated to the N-terminus of an Aib-containing foldamer carrying the C-terminal FibTEG ss-NMR conformational reporter. The resulting oligomer **4** (Fig. 3) carries ^{19}F labels at both the N and C termini, allowing parallel monitoring by ^{19}F ss-NMR of both configurational *E/Z* photoswitching in the azobenzene unit and consequent global conformational population switching of the foldamer. (The similar behavior of a Phe-containing analogue is described in fig. S17).

Foldamer **4** was equilibrated in the dark to a >99:1 *E/Z* ratio and embedded into the DOPC membrane phase using the procedure described earlier, but minimizing exposure to light. The ^{19}F ss-NMR spectrum (Fig. 3A) of the membrane-embedded foldamer showed a fluoroarene signal at δ −126 ppm, accompanied by two equally populated but unequally broadened (due to chemical shift anisotropy differences) signals in the region of δ −234 ppm. The single signal at δ −126 ppm confirmed that the azobenzene was still a single geometrical isomer after incorporation into the lipid bilayer. The appearance of two signals at δ −234 ppm, separated by ~1 ppm (Fig. 3A), indicates that the foldamer is in its 'on' state, with one of the equilibrating screw-sense conformers of the helical structure preferentially populated. Analogy with behavior of related Aib foldamers in solution suggests that the preferred conformational state is left-handed and accounts for approximately 60 to 65% of the equilibrium population (*43*).
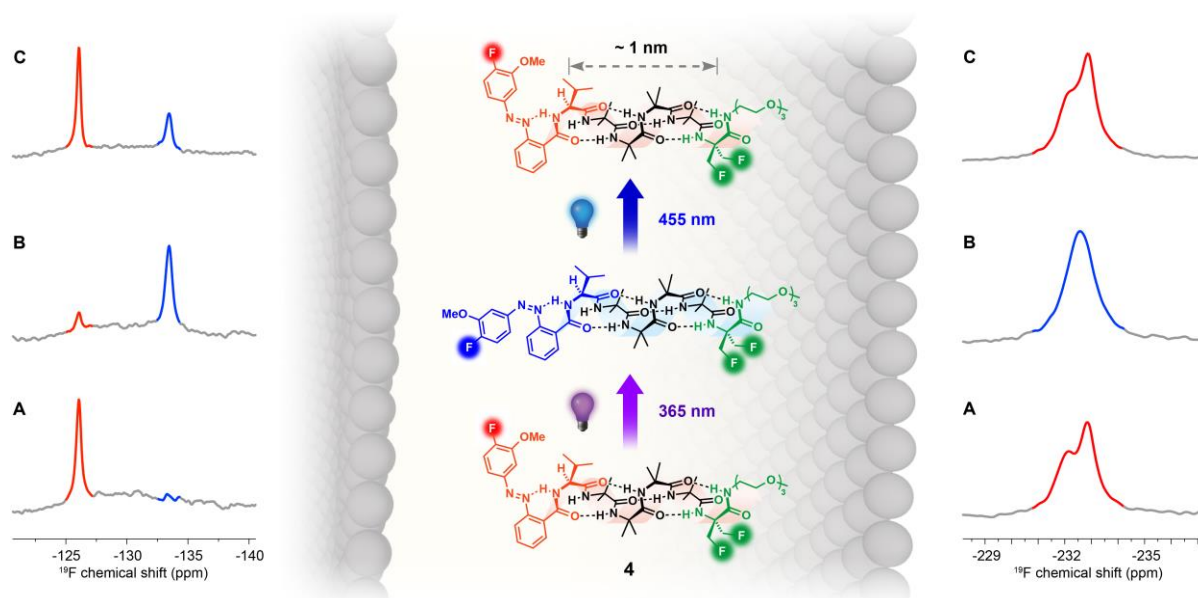
Fig. 3. Conformational switching of **4** by irradiation in a DOPC phospholipid bilayer (5% w/w). Molecular dimensions, but not necessarily orientation, of **4** are shown in proportion to the thickness of the bilayer, with the bilayer boundary indicated by grey balls representing the phosphate head-groups. Portions of the ^{19}F ss-NMR spectra corresponding to the N-terminal fluoroarene substituent (δ −125 to −140 ppm, left) and the C-terminal FibTEG reporter (δ −230 to −235 ppm, right) are shown as well. (**A**) Dark-equilibrated sample (>99:1 *E*/*Z* azobenzene ratio); (**B**) the same sample after irradiation at 365 nm (14:86 *E*/*Z* ratio) and (**C**) after subsequent irradiation at 455 nm (69:31 *E*/*Z* ratio).

The suspension of MLVs containing foldamer (*E*)-**4** was then transferred to a quartz cuvette and illuminated using an LED of wavelength 365 nm (fig. S11). After 5 minutes, the phospholipid mixture was spun out from the cuvette and directly loaded into the MAS rotor. The ^{19}F ss-NMR spectrum (Fig. 3B) now revealed relative intensities of 14:86 for the signals corresponding to the *E* and *Z* azobenzenes, indicating substantial switching of the azobenzene geometry from *E* to *Z* within the phospholipid bilayer. Simultaneously, the pair of signals arising from the FibTEG reporter had collapsed into a broad singlet (Fig. 3B). This indicates that the photo-induced change in geometry at the N-terminal azobenzene had induced a global conformational switch into an 'off' state, in which an approximately equal population of left and right handed screw-sense conformers is detected by the C-terminal reporter.

This *Z*-rich sample of **4** was transferred back into a quartz cuvette and illuminated a second time, with light of wavelength 455 nm, and again a ss-NMR sample was prepared using this now twice-illuminated, membrane-bound oligomer. This longer wavelength illumination changed back the *E/Z* isomer population to a 69:31 ratio and restored the initial peak separation of the FibTEG reporter (Fig. 3C). This second irradiation at longer wavelength thus switched the foldamer back into its 'on' state, reinstating its original conformational preference for a preferred screw sense, and demonstrating the reversibility of the photoswitching process (see also fig. S16 for multiple, reversible photoswitching cycles).

No changes were evident in the FibTEG region of the ^{19}F ss-NMR spectrum when a similar illumination procedure was applied to an azobenzene-free foldamer, nor using

azobenzene-capped but achiral foldamer after irradiation at 365, 405 or 455 nm (see fig. S14 and S15). The slow Z to E thermal relaxation exhibited by the fluorinated azobenzene-valine moiety in CD$_3$OD solution ($t_{1/2}$ = 64 h for **1d**, fig. S6) became only slightly faster in the phospholipid bilayer ($t_{1/2} \approx$ 44 h for both **4** and **5**, fig. S19-20). This proved particularly helpful for the purposes of this study, given the acquisition time required (0.5 to 1 h) for each ss-NMR spectrum.

With the aim of transmitting conformational information over multi-nanometer distances comparable with the reach of the photo-induced conformational changes in rhodopsin that underpin the biochemistry of vision (*44*), we also studied foldamers with a much more extended helical structure. Foldamer **5** was synthesized, in which the azobenzene chromophore was separated from the FibTEG reporter by eight Aib residues, or about three turns of a 3$_{10}$ helix, corresponding to a distance of 2 nm (*45*), a distance commensurate the hydrophobic thickness of a DOPC bilayer (Fig 4A) (*42*). (A related phenylalanine-containing foldamer is reported fig. S18). Preliminary ^{19}F NMR studies in CDCl$_3$ (fig. S8) indicated that the rate of exchange between conformational states is slower in these longer homologues ($T_c \sim$ +35 °C, indicating a rate of <6000 s^{-1} at room temperature (*46*)). After insertion into the DOPC bilayer but before irradiation, integration of the ^{19}F ss-NMR signals at $\sim \delta$ −130 ppm indicated that **5** exists as a 92:8 mixture of E and Z geometrical isomers. Foldamer **5** showed two FibTEG NMR signals in the region of δ −234 ppm separated by 4.0 ppm (Fig. 4A). The membrane-embedded foldamers were irradiated for 7 minutes with light of wavelength 365 nm, which switched the azobenzene chromophore to an 18:82 E/Z geometrical ratio, and simultaneously caused a marked change in the FibTEG reporter signal, increasing the separation of the peaks to 5.4 ppm (Fig. 4B). A second period of illumination at 455 nm switched back the population of azobenzene geometrical isomers to a 71:29 E/Z ratio, and returned the chemical shift separation to its initial value (Fig. 4C). As in CDCl$_3$ solution, the spectroscopic responses of **5** in the membrane phase are characteristic of slower exchange between screw-sense conformations (they are in intermediate exchange on the NMR timescale), which at this stage in the work prevents us quantifying the relative populations of the conformational states. The results demonstrate that light-induced configurational switching at one location in extended membrane-bound synthetic molecules induces local changes in structure that propagate through the oligomers to induce global changes in conformation, causing a change in conformational populations that is detected by spatially remote reporters.
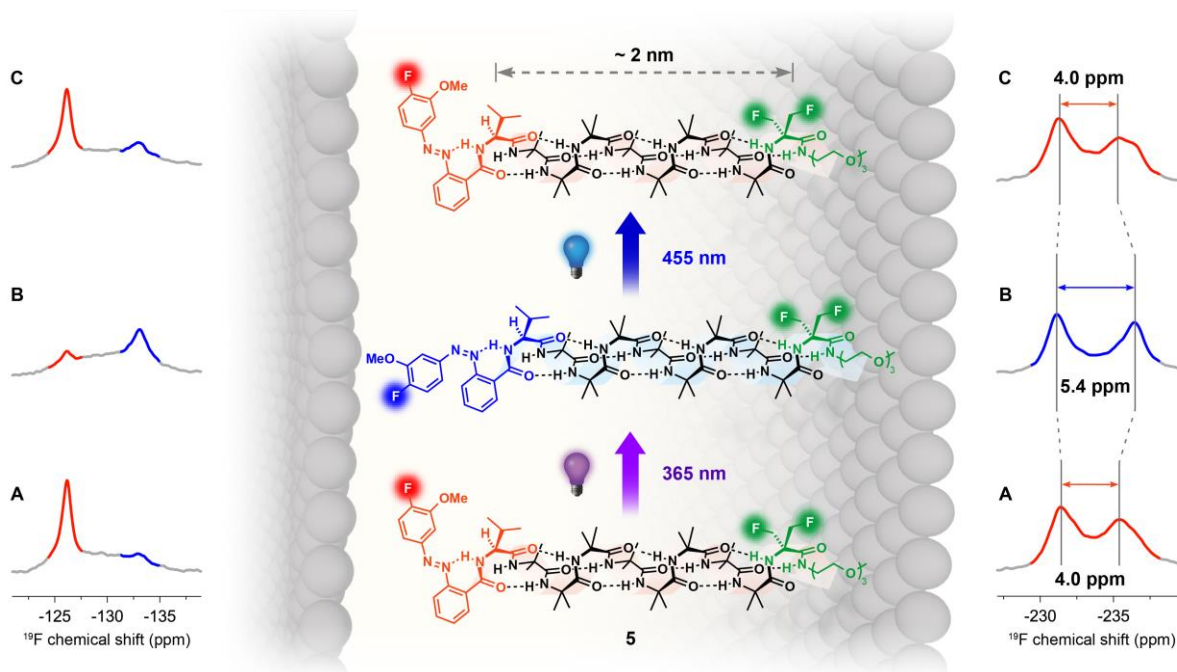
Fig. 4. Conformational switching of **5** by irradiation in a DOPC phospholipid bilayer (5% w/w). Molecular dimensions, but not necessarily orientation, of **5** are shown in proportion to the thickness of the bilayer, with the bilayer boundary indicated by grey balls representing the phosphate head-groups. Portions of the ^{19}F ss-NMR spectra corresponding to the N-terminal fluoroarene substituent (δ −125 to −135 ppm, left) and the C-terminal FibTEG reporter (δ −230 to −240 ppm, right) are shown as well. (**A**) Dark-equilibrated sample (92:8 *E/Z* azobenzene ratio); (**B**) the same sample after irradiation at 365 nm (18:82 *E/Z* ratio) and (**C**) after subsequent irradiation at 455 nm (71:29 *E/Z* ratio).

We have shown that the dynamic control over the conformational behavior of foldamers in solution may be replicated in a phospholipid bilayer. We envisage that replacement of the spectroscopic reporter with a catalytic or binding site in related switchable oligomers should allow photoswitchable changes in conformation to lead to stimulated release of a chemical messenger, or catalytic formation of a secondary messenger to be up- or downregulated (*47*). Incorporation of such switchable functional molecules into membranes would allow localized, photoinduced chemical changes to be translated into chemical responses in the lumen of artificial vesicles, or even the controlled release or uptake of a chemical signal in the cytosol of individual live cells. The work demonstrates that simplified synthetic molecules may be designed to display the essential functions of much more complex, evolved biomolecules.

Full Reference List

1.   J. Broichhagen, D. Trauner, The *in vivo* chemistry of photoswitched tethered ligands. *Curr. Op. Chem. Biol.* **21**, 121−127 (2014).
2.   R. Göstl, A. Senf, S. Hecht, Remote-controlling chemical reactions by light: towards chemistry with high spatio-temporal resolution. *Chem. Soc. Rev.* **43**, 1982−1996 (2014).

3. B. L. Feringa, W. E. Browne, Eds., *Molecular Switches* (Wiley-VCH, Weinheim, 2011) [second edition].

4. W. J. De Grip, K. J. Rothschild, in *Molecular Mechanisms of Visual Transduction*, D. G. Stavenga, W. J. De Grip, E. N. Pugh Jr., Eds. (Elsevier, Amsterdam, 2000), pp. 1−54.

5. R. Nygaard *et al.*, The dynamic process of β_2-adrenergic receptor activation. *Cell* **152**, 532−542 (2013).

6. K. Henzler-Wildman, D. Kern, Dynamic personalities of proteins. *Nature* **450**, 964−972 (2007).

7. F. Hu, W. Luo, M. Hong, Mechanisms of proton conduction and gating by influenza M2 proton channels from solid-state NMR, *Science* **330**, 505−508 (2010).

8. S. H. Gellman, Foldamers: a manifesto. *Acc. Chem. Res.* **31**, 173−180 (1998).

9. C. Toniolo, E. Benedetti, The polypeptide 3_{10}-helix. *Trends Biochem. Sci.* **16**, 350−353 (1991).

10. C. Toniolo, H. Brückner, Eds., *Peptaibiotics* (Wiley-VCH, Weinheim, 2009).

11. H. M. D. Bandara, S. C. Burdette, Photoisomerization in different classes of azobenzene. *Chem. Soc. Rev.* **41**, 1809−1825 (2012).

12. M. De Poli *et al.*, Engineering the structure of an N-terminal β-turn to maximize screw-sense preference in achiral helical peptide chains. *J. Org. Chem.* **79**, 4659−4675 (2014).

13. G. Shanmugan, P. L. Polavarapu, Structure of Aβ(25–35) peptide in different environments. *Biophys. J.* **87**, 622−630 (2004).

14. S. J. Pike, V. Diemer, J. Raftery, S. J. Webb, J. Clayden, Designing foldamer–foldamer interactions in solution: the roles of helix length and terminus functionality in promoting the self-association of aminoisobutyric acid oligomers. *Chem. Eur. J.* **20**, 15981−15990 (2014).

15. Electron-donating groups *para* to the azo linkage were avoided as they are known to promote fast thermal relaxation to the *E* isomer. See (*16*).

16. N. Nishimura *et al.*, Thermal *cis*-to-*trans* isomerization of substituted azobenzenes. II. Substituents and solvent effects. *Bull. Chem. Soc. Jpn.* **49**, 1381−1387 (1976).

17. B. A. F. Le Bailly, L. Byrne, V. Diemer, M. Foroozandeh, G. A. Morris, J. Clayden, Flaws in foldamers: conformational uniformity and signal decay in achiral helical peptide oligomers, *Chem. Sci.*, **6**, 2313−2322 (2015).

18. F. Gerson, E. Heilbronner, A. van Veen, B. M. Wepster, Elektronenstruktur und physikalisch-chemische eigenschaften von azo-verbindungen. Teil VIII: die konjugaten säuren des *trans*- und des *cis*-azobenzols. *Helv. Chim. Acta* **43**, 1889−1898 (1960).

19. M. J. Duer, *Introduction to Solid-State NMR Spectroscopy* (Blackwell, Oxford, 2004).

20. D. Huster, Solid-state NMR spectroscopy to study protein–lipid interactions. *Biochim. et Biophys. Acta (BBA) - Molecular and Cell Biology of Lipids* **1841**, 1146−1160 (2014).

21. E. Strandberg, A. S. Ulrich, NMR methods for studying membrane-active antimicrobial peptides. *Concepts Magn. Reson. A* **23**, 89−120 (2004).

22. M. Hong, Y. Zhang, F. Hu, Membrane protein structure and dynamics from NMR spectroscopy. *Annu. Rev. Phys. Chem.* **63**, 1−24 (2012).

23. E. D. Watt, C. M. Rienstra, Recent advances in solid-state nuclear magnetic resonance techniques to quantify biomolecular dynamics. *Anal. Chem.* **86**, 58−64 (2014).

24. L. A. Baker, M. Baldus, Characterization of membrane protein function by solid-state NMR spectroscopy, *Curr. Op. Struct. Biol.* **27**, 48−55 (2014).

25. C. Aisenbrey, N. Pendem, G. Guichard, B. Bechinger, Solid state NMR studies of oligourea foldamers: interaction of ^{15}N-labelled amphiphilic helices with oriented lipid membranes. *Org. Biomol. Chem.* **10**, 1440−1447 (2012).

26. A. V. Struts, U. Chawla, S. M. Perera, M. F. Brown, Investigation of rhodopsin dynamics in its signaling state by solid-state deuterium NMR spectroscopy. *Methods Mol. Biol.* **1271**, 133−158 (2015).

27. T. Nagao *et al.*, Structure and orientation of antibiotic peptide alamethicin in phospholipid bilayers as revealed by chemical shift oscillation analysis of solid state nuclear magnetic resonance and molecular dynamics simulation. *Biochim Biophys Acta* **1848**, 2789−2798 (2015).

28. T. Polenova, R. Gupta, A. Goldbourt, Magic angle spinning NMR spectroscopy: a versatile technique for structural and dynamic analysis of solid-phase systems. *Anal. Chem.* **87**, 5458−5469 (2015).

29. A. Ramamoorthy, J. Xu, 2D ^{1}H/^{1}H RFDR and NOESY NMR experiments on a membrane-bound antimicrobial peptide under magic angle spinning. *J. Phys. Chem. B* **117**, 6693−7000 (2013).

30. K. Koch, S. Afonin, M. Ieronimo, M. Berditsch, A. S. Ulrich, in *Topics in current Chemistry*, J. C. C. Chan, Ed., (Springer, Berlin, 2012), vol. 306, pp. 89−118.

31. Y. Su, W. F. DeGrado, M. Hong, Orientation, dynamics, and lipid interaction of an antimicrobial arylamide investigated by ^{19}F and ^{31}P solid-state NMR spectroscopy. *J. Am. Chem. Soc.* **132**, 9197−9205 (2010).

32. J. K. Williams *et al.*, Drug-induced conformational and dynamical changes of the S31N mutant of the influenza M2 proton channel investigated by solid-state NMR. *J. Am. Chem. Soc.* **135**, 9885−9897 (2013).

33. N. Joh, T. Wang, M. Bhate, R. Acharya, Y. Wu, M. Grabe, M. Hong, G. Grigoryan, W.F. DeGrado, De novo design of a transmembrane Zn(II) transporting four-helix bundle. *Science* **346**, 1520−1524 (2014).

34. S. J. Pike *et al.*, Diastereotopic fluorine substituents as ^{19}F NMR probes of screw-sense preference in helical foldamers. *Org. Biomol. Chem.* **11**, 3168−3176 (2013).

35. P. Wadhwani, E. Strandberg, in *Fluorine in Medicinal Chemistry and Chemical Biology*, I. Ojima, Ed., (Wiley, Chichester, 2009) pp. 463−494.

36. S. Mazeres, V. Schram, J.-F. Tocanne, A. Lopez, 7-nitrobenz-2-oxa-1,3-diazole-4-yl-labeled phospholipids in lipid membranes: differences in fluorescence behavior. *Biophys. J.* **71**, 327−335 (1996).

37. F. Szoka, D. Papahadjopoulos, Comparative properties and methods of preparation of lipid vesicles (liposomes). *Ann. Rev. Biophys. Bioeng.* **9**, 467−508 (1980).

38. D. E. Warschawski *et al.*, Choosing membrane mimetics for NMR structural studies of transmembrane proteins. *Biochim. Biophys. Acta, Biomembr.* **1808**, 1957−1974 (2011).

39. J. H. Davis, M. Auger, R. S. Hodges, High resolution ^{1}H nuclear magnetic resonance of a transmembrane peptide. *Biophys. J.* **69**, 1917−1932 (1995).

40. M. Bouchard, J. H. Davis, M. Auger, High-speed magic angle spinning solid-state ^{1}H nuclear magnetic resonance study of the conformation of gramicidin A in lipid bilayers. *Biophys. J.* **69**, 1933−1938 (1995).

41. A. V. Filippov, A. M. Khakimov, B. V. Munavirov, ^{31}P NMR Studies of phospholipids. *Ann. Rep. NMR Spectr.* **85**, 27-92 (2015).

42.   N. Kučerka, J. F. Nagle, J. N. Sachs, S. E. Feller, J. Pencer, A. Jackson, J. Katsaras, Lipid bilayer structure determined by the simultaneous analysis of neutron and X-ray scattering data. *Biophys J.* **95**, 2356–2367 (2008).

43.   R. A. Brown, T. Marcelli, M. De Poli, J. Solà, J. Clayden, Induction of unexpected left-handed helicity by an N-terminal L-amino acid in an otherwise achiral peptide chain. *Angew. Chem. Int. Ed.* **51**, 1395−1399 (2012).

44.   H.-W. Choe *et al.*, Crystal structure of metarhodopsin II. *Nature* **471**, 651−655 (2011)

45.   R. Gessmann, H. Brückner, K. Petratos, Three complete turns of a 3_{10}-helix at atomic resolution: the crystal structure of Z-(Aib)$_{11}$-O*t*Bu. *J. Pept. Sci.* **9**, 753−762 (2003).

46.   R.-P. Hummel, C. Toniolo, G. Jung, Conformational transitions between enantiomeric 3_{10} helices, *Angew. Chemie Int. Ed.* **26**, 1150−1152 (1987).

47.   B. A. F. Le Bailly, L. Byrne, J. Clayden, Refoldable foldamers: global conformational switching by deletion or insertion of a single hydrogen bond. *Angew. Chemie Int. Ed.* **55**, 2132-2136 (2016).

SM references:

48.   G. M. Badger, R. J. Drewer, G. E. Lewis, Photochemical reactions of azo compounds. III. Photochemical cyclodehydrogenations of substituted azobenzenes. *Austr. J. Chem.* **17**, 1036−1049 (1964).

49.   T. W. M. Spence, G. Tennant, The chemistry of nitro-compounds. Part II. The scope and mechanism of the base-catalysed transformations of some N,N-disubstituted o-nitrobenzamides. *J. Chem. Soc. Perkin Trans.* **1**, 97−102 (1972).

50.   S. Keiper, J. S. Vyle, Reversible photocontrol of deoxyribozyme-catalyzed RNA cleavage under multiple-turnover conditions. *Angew. Chem. Int. Ed.* **45**, 3306−3309 (2006).

51.   A. J. Harvey, A. D. Abell, Azobenzene-containing, peptidyl α-ketoesters as photobiological switches of α-chymotrypsin. *Tetrahedron* **56**, 9763 (2000).

52.   F. Tibiletti *et al.*, One-pot synthesis of meridianins and meridianin analogues via indolization of nitrosoarenes. *Tetrahedron* **66**, 1280−1288 (2010).

53.   A. Defoin, Simple preparation of nitroso benzenes and nitro benzenes by oxidation of anilines with H_2O_2 catalysed with molybdenum salts. *Synthesis* **5**, 706−710 (2004).

54.   R. Jurok *et al.*, Planar chiral flavinium salts: synthesis and evaluation of the effect of substituents on the catalytic efficiency in enantioselective sulfoxidation reactions. *Eur. J. Org. Chem.* **2013**, 7724−7738 (2013).

55.   K. Dan, N. Bose, S. Ghosh, Vesicular assembly and thermo-responsive vesicle-to-micelle transition from an amphiphilic random copolymer. *Chem. Comm.* **47**, 12491−12493 (2011).

56.   J. Clayden, A. Castellanos, J. Solà, G. A. Morris, Quantifying end-to-end conformational communication of chirality through an achiral peptide chain. *Angew. Chem. Int. Ed.* **48**, 5962 (2009).

57.   L. Byrne *et al.*, Foldamer-mediated remote stereocontrol: >1,60 asymmetric induction. *Angew. Chem. Int. Ed.* **53**, 151 (2014).

58.   J. Solà, G. A. Morris, J. Clayden, Measuring screw-sense preference in a helical oligomer by comparison of ^{13}C NMR signal separation at slow and fast exchange. *J. Am. Chem. Soc.* **133**, 3712 (2011).

59. W. M. Yau, W. C. Wimley, K. Gawrisch, S. H. White, The preference of tryptophan for membrane interfaces. *Biochemistry* **37**, 14713 (1998).

Supplementary Materials:

Materials and Methods
Supplementary text, images and data
Figs. S1 to S21
Tables S1 to S9
References (*48-59*)